

# Use of an Unmanned Aircraft System to Quantify NO<sub>x</sub> Emissions from a Natural Gas Boiler

Brian Gullett<sup>1</sup>, Johanna Aurell<sup>2</sup>, William Mitchell<sup>1</sup>, Jennifer Richardson<sup>3</sup>

<sup>1</sup>US Environmental Protection Agency, Office of Research and Development, Research Triangle Park, North Carolina, 27711, USA; <sup>2</sup>University of Dayton Research Institute, Dayton, Ohio, 45469-7532, USA; <sup>3</sup>The Dow Chemical Company, Midland, Michigan, 48667, USA.

*Correspondence to:* Brian Gullett (gullett.brian@epa.gov)

## Abstract

Aerial emission sampling of four natural gas boiler stack plumes was conducted using an unmanned aerial system (UAS) equipped with a light-weight sensor/sampling system (the “Kolibri”) for measurement of nitrogen oxide (NO), and nitrogen dioxide (NO<sub>2</sub>), carbon dioxide (CO<sub>2</sub>), and carbon monoxide (CO). Flights (n = 22) ranged from 11 to 24 minutes duration at two different sites. The UAS was maneuvered into the plumes with the aid of real-time CO<sub>2</sub> telemetry to the ground operators and, at one location, a second UAS equipped with an infrared/visible camera. Concentrations were collected and recorded at 1 Hz. The maximum CO<sub>2</sub>, CO, NO, and NO<sub>2</sub> concentrations in the plume measured were 10,000 ppm, 7 ppm, 27 ppm, and 1.5 ppm, respectively. Comparison of the NO<sub>x</sub> emissions between the stack continuous emission monitoring systems and the UAS/Kolibri for three boiler sets showed an average of 5.6 % and 3.5 % relative percent difference for the run-weighted and carbon-weighted average emissions, respectively. To our knowledge, this is the first evidence for the accuracy performance of UAS-based emission factors against a source of known strength.

Keywords: Emissions, natural gas, boiler, unmanned aircraft system, drone, continuous emission monitoring



TOC Art

## 26 1 Introduction

27 Aerial measurement of plume concentrations is a new field made possible by advances in Unmanned Aircraft  
28 Systems (UAS, or “drones”), miniature sensors, computers, and small batteries. The use of a UAS platform for  
29 environmental sampling has significant advantages in many scenarios in which access to environmental samples are  
30 limited by location or accessibility. Hazards to equipment and personnel can also be minimized by the mobility of  
31 the UAS as well as their ability to be remotely operated away from hazardous sources. UAS-based emission  
32 samplers have been used for measurement of area source gases (Neumann et al., 2013; Rosser et al., 2015; Chang et  
33 al., 2016; Li et al., 2018), point source gases (Villa et al., 2016), aerosols (Brady et al., 2016), black carbon particles  
34 (Craft, 2014), volcanic pollutants (Mori et al., 2016), particle mass (Peng et al., 2015), and particle number  
35 concentrations (Villa et al., 2016).

36 UAS-based emission measurements are particularly suited for area source measurements of fires and can be used to  
37 determine emission factors, or the mass amount of a pollutant per unit of source operation, such as mass of  
38 particulate matter (PM) per mass of fuel (e.g., biomass) burned. These values can be converted into emission rates,  
39 such as mass of pollutant per unit of energy (e.g., g NO<sub>x</sub> kJ<sup>-1</sup>). These determinations typically rely on the carbon  
40 balance method in which the target pollutant is co-sampled with the major carbon species present and, with  
41 knowledge of the source’s fuel (carbon) composition, the pollutant to fuel ratio or an emission rate/factor, can be  
42 calculated.

43 For internal combustion sources that have a process emission stack, downwind plume sampling can use the same  
44 method. When combined with the source fuel supply rate and stack flow rates (to determine the dilution rate),  
45 measurements comparable to extractive stack sampling may be possible. To our knowledge, determination of  
46 emission factors from a stack plume using a UAS-borne sampling system has not previously been demonstrated. The  
47 goal of this effort was to compare NO<sub>x</sub> measurements obtained by UAS-borne emission samplers with those from  
48 concurrent CEM measurements. While not necessarily obviating the need for CEMs for regulatory compliance, the  
49 use of UAS-based measurements could provide a safe and fast method of checking emissions that does not require  
50 personnel and equipment to access elevated stacks for periodic CEM verification. More importantly, however, the  
51 comparison of UAS-based emission measurements against a source of known CEM-determined concentration  
52 allows the accuracy of this new type of measurement to be assessed. Demonstrating the efficacy of these  
53 measurements would then open their applicability to other less understood sources that are not amenable to  
54 conventional CEM sampling, such as open fires, industrial flares, and gas releases.

55 The feasibility of downwind plume sampling using a sensor-equipped UAS was tested on industrial boilers at the  
56 Dow Chemical Company (Dow) facilities in Midland, Michigan (MI) and St. Charles, Louisiana (LA). The sensor  
57 system was designed and built by the EPA’s Office of Research and Development and the UAS was owned and  
58 flown by the Dow Corporate Aviation Group. To determine the comparative accuracy of the measurements, the  
59 UAS-based emission factor was compared with the stack continuous emission monitoring systems (CEMS). The  
60 target pollutants were nitrogen oxide (NO) and nitrogen dioxide (NO<sub>2</sub>) to mimic the stack CEMS measurement  
61 methods. Carbon as carbon dioxide (CO<sub>2</sub>) and carbon monoxide (CO) were measured on the UAS for the carbon  
62 balance method.

## 63 2 Materials and Method

64 Plume sampling tests were conducted on two natural-gas-fired industrial boilers located at Dow’s Midland,  
65 Michigan and St. Charles, Louisiana facilities. The Midland boilers are firetube type boilers using low pressure  
66 utility supplied natural gas. They are equipped with low NO<sub>x</sub> burners and utilize flue gas recirculation to reduce  
67 stack NO<sub>x</sub> concentrations. The Midland facility burned natural gas with a higher heating value (HHV) of 9,697 kcal  
68 m<sup>-3</sup> (1089 British Thermal Unit (BTU)/ft<sup>-3</sup>). The two tested stacks are 14 m above ground level and 7 m apart. To

69 avoid sampling overlapping plumes, only a single boiler was operating during the testing. The St. Charles boilers are  
 70 D-type water package boilers using natural gas fuels (high pressure fuel gas (HPFG) and low pressure off-gas  
 71 (LPOG)). They are equipped with low NO<sub>x</sub> burners with flue gas recirculation to reduce stack NO<sub>x</sub> concentrations.  
 72 The boiler stacks are about 20 m apart and reach over 20 m in height above ground level. The St. Charles facility  
 73 burned natural gas under steady state conditions with a composition of 77.12 % CH<sub>4</sub>, 2.01 % C<sub>2</sub>H<sub>6</sub>, and 19.91 % H<sub>2</sub>  
 74 and a HHV of 7,845 kcal m<sup>-3</sup> (881 BTU ft<sup>-3</sup>). Both boilers were operational during aerial sampling, but the wind  
 75 direction and UAS proximity to the target stack precluded co-mingling of the plumes.

76 Air sampling was accomplished with an EPA/ORD-developed sensor/sampler system termed the “Kolibri”. The  
 77 Kolibri consists of real-time gas sensors and pump samplers to characterize a broad range of gaseous and particle  
 78 pollutants. This self-powered system has a transceiver for data transmission and pump control (Xbee S3B, Digi  
 79 International, Inc., Minnetonka, MN, USA) from the ground-based operator. For this application, gas concentrations  
 80 were measured using electrochemical cells for CO, NO, and NO<sub>2</sub> and a non-dispersive infrared (NDIR) cell for CO<sub>2</sub>  
 81 (Table 1). All sensors were selected for their applicability to the anticipated operating conditions of concentration  
 82 level and temperature as well as for their ability to rapidly respond to changing plume concentrations due to  
 83 turbulence and entrainment of ambient air. Each sensor underwent extensive laboratory testing to verify  
 84 performance and suitability prior to selection for the Kolibri. Tests included sensor performance (linearity, drift,  
 85 response time, noise, detection limits) in response to anticipated field temperatures, pressure, humidity, and  
 86 interferences. Additional information from the manufacturers on sensor performance is available from the links in  
 87 Table 1. In anticipation of temperatures as low as 0°C at the Midland site and to avoid daily temperature  
 88 fluctuations, insulation was added to the Kolibri frame and the sampled gases were preheated prior to the sensor  
 89 with the use of a heating element and micro fan inside the Kolibri. All sensors were calibrated before each sampling  
 90 day under local ambient conditions. After sampling was completed, the sensors were similarly tested to assess  
 91 potential drift.

92 Concentration data were stored by the Kolibri using a Teensy USB-based microcontroller board (Teensy 3.2, PJRC,  
 93 LLC., Sherwood, OR, USA) with an Arduino-generated data program and SD data card. All four sensors underwent  
 94 pre- and post-sampling two- or three-point calibration using gases (Calgasdirect Inc., Huntington Beach, CA, USA)  
 95 traceable to National Institute of Standards and Technology (NIST) standards.

96  
 97 **Table 1. UAS/Kolibri Target Analytes and Methods**

Analyte	Instrument, Manufacturer’s Data Link	Frequency	Cal. Gases (ppm) Midland	Cal Gases (ppm) St. Charles
CO <sub>2</sub>	SenseAir CO <sub>2</sub> Engine K30, NDIR <sup>a</sup> <a href="https://www.co2meter.com/products/k-30-co2-sensor-module">https://www.co2meter.com/products/k-30-co2-sensor-module</a>	Continuous, 1 Hz <sup>b</sup>	408, 990	392, 996, 5890
CO	E2v EC4-500-CO, Electrochemical cell <a href="https://www.sgxsensortech.com/content/uploads/2014/07/EC4-500-CO1.pdf">https://www.sgxsensortech.com/content/uploads/2014/07/EC4-500-CO1.pdf</a>	Continuous, 1 Hz	0 <sup>c</sup> , 9.67, 50.6	0, 9.9, 51.8
NO	NO-D4, Electrochemical cell <a href="http://www.alphasense.com/WEB1213/wp-content/uploads/2013/10/NOD4.pdf">http://www.alphasense.com/WEB1213/wp-content/uploads/2013/10/NOD4.pdf</a>	Continuous, 1 Hz	0, 2.1, 41.4	0, 2.1, 40.4
NO <sub>2</sub>	NO2-D4, Electrochemical cell <a href="http://www.alphasense.com/WEB1213/wp-content/uploads/2020/09/NO2-D4.pdf">http://www.alphasense.com/WEB1213/wp-content/uploads/2020/09/NO2-D4.pdf</a>	Continuous, 1 Hz	0, 2.1, 10.4	0, 1.9, 10.4

98 <sup>a</sup>Non-dispersive infrared. <sup>b</sup>Hz – hertz. <sup>c</sup>Zero (0) cal gas = air.

100 The NO sensor (NO-D4) is an electrochemical gas sensor (Alphasense, Essex, UK) which measures concentration  
101 by changes in impedance. The sensor has a detection range of 0 to 100 ppm with resolution of < 0.1 RMS noise  
102 (ppm equivalent) and linearity within  $\pm 1.5$  ppm error at full scale. The NO-D4 was tested to have a response time to  
103 95 % of concentration ( $T_{95\%}$ ) of  $6.3 \pm 0.52$  seconds and a noise level of 0.027 ppm. The temperature and relative  
104 humidity (RH) operating range is 0 to +50 °C and 15 to 90 % RH, respectively.

105 The NO<sub>2</sub> sensor (NO2-D4) is an electrochemical gas sensor (Alphasense, Essex, UK) which likewise measures by  
106 impedance changes. It has a NO<sub>2</sub> detection range of 0-10 ppm with resolution of 0.1 RMS noise (ppm equivalent)  
107 and linearity error of 0 to 0.6 ppm at full scale. Its  $T_{95\%}$  was measured as  $32.3 \pm 3.8$  seconds with a noise level of  
108 0.015 ppm. The temperature and RH operating range is 0 to +50 °C and 15 to 90 % RH, respectively.

109 Laboratory calibration testing prior to field measurements on both the NO-D4 and NO2-D4 sensors outputs showed  
110 their responses to be linearly proportional ( $R^2 > 0.99$ ) over the range of 4- and 5-point calibration gas  
111 concentrations. The response times of both sensors were derived using the maximum reference concentration of  
112 47.81 ppm for NO and 10.46 ppm of NO<sub>2</sub>. The times to reach 95% of the reference concentration,  $t_{95}$ , were 6.3 and  
113 32.3 sec (RSD (8.2% and 11.8%), respectively, for the NO-D4 and NO2-D4 sensors. These response times are both  
114 shorter than those measured simultaneously in the laboratory by a CEM (Ametek 9000<sup>RM</sup>, Pittsburgh, PA, USA) at  
115 37 and 50 sec, respectively, for NO and NO<sub>2</sub>.

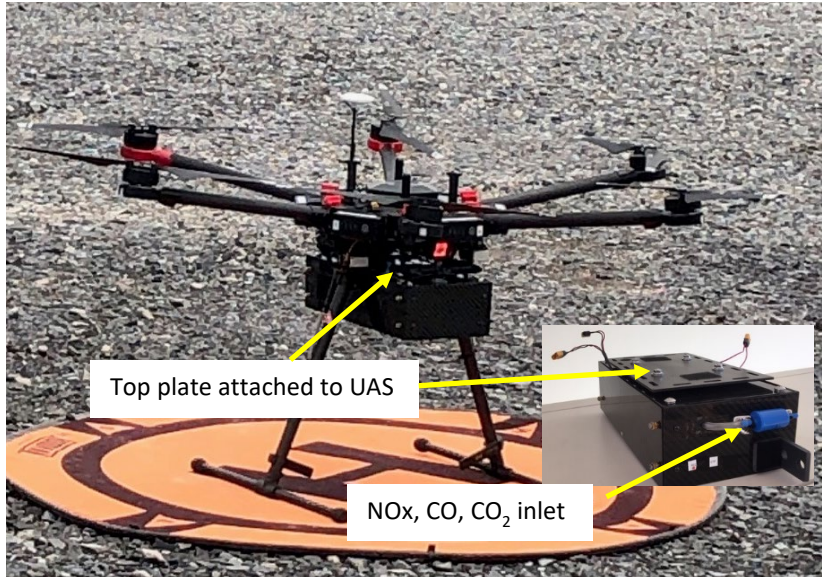
116 The CO<sub>2</sub> sensor (CO<sub>2</sub> Engine® K30 Fast Response, SenseAir, Delsbo, Sweden) is an NDIR gas sensor and the  
117 voltage output is linear from 400 to 10,000 ppm. The temperature and RH operating range is 0 to +50 °C and 0 to 90  
118 % RH, respectively. The CO<sub>2</sub>-K30 sensor was measured to have a  $t_{95\%}$  response time at 6000 ppm CO<sub>2</sub> of  $9.0 \pm 0.0$   
119 seconds and having a noise level of 1.6 ppm. The response time was 4 sec longer than compared to CO<sub>2</sub> measured  
120 by a portable gas analyzer (LI-820, LI-COR Biosciences, Lincoln, NE, USA). The sensor and the LI-820 showed  
121 good agreement as the measurements showed a  $R^2$  of 0.99 and a slope of 1.01.

122 The CO sensor (e2V EC4-500-CO, SGX Sensortech Ltd, High Wycombe, Buckinghamshire UK) is described more  
123 fully elsewhere (Aurell et al., 2017; Zhou et al., 2017). In previous sensor evaluation tests with laboratory biomass  
124 burns (Zhou et al., 2017) with CO ranging between 0 and 250 ppm, the sensor was compared to simultaneous  
125 measurements by a CO CEM (CAI Model 200, California Analytical Instruments Inc., Orange, CA, USA). The  
126 concentration measurements had an  $R^2 = 0.98$  and a slope of 1.04, indicating the level of agreement between the two  
127 devices. The  $t_{90}$  was measured as 18 s while comparison of the time-integrated CO concentration differences with  
128 the CAI-200, rated at  $t_{90} < 1$  s, were only 4.9%.

129  
130 Variations of the Kolibri sampling system allow for measurement of additional target pollutants. These include  
131 particulate matter (PM), polycyclic aromatic hydrocarbons (PAHs), volatile organic compounds (VOCs) including  
132 carbonyls, energetics, chlorinated organics, metals from filter analyses, and perchlorate (Aurell et al., 2017; Zhou et  
133 al., 2017).

134 At both facilities the aviation team from Dow flew their DJI Matrice 600 UAS, a six-motor multicopter  
135 (hexacopter), into the plumes with EPA/ORD's Kolibri sensor/sampler system attached to the undercarriage (Figure  
136 1). In this configuration of sensors, the Kolibri system weighed 2.4 kg. Typical flight elevations at Midland and St.  
137 Charles were 21 and 32 m above ground level (AGL), respectively, and flight durations ranged from 9 to 24 min.  
138 At the St. Charles location, the UAS pilot was approximately 100 m from the center point of the two stacks, easily  
139 allowing for line of sight operation. A telemetry system on the Kolibri provided real time CO<sub>2</sub> concentration and  
140 temperature data to the Kolibri operator who in turn advised the pilot on the optimum UAS location.

141 CEMS on the boiler stacks produced a continuous record of NO<sub>x</sub> emission and O<sub>2</sub> concentrations. Stack and CEMS  
 142 types located at the Midland and St. Charles facilities are shown in Table 2. The stack NO<sub>x</sub> analyzer uses a  
 143 chemiluminescence measurement with a photomultiplier tube and is capable of split concentration range operation:  
 144 Low (0-180 ppm) and High (0-500 ppm). Its response time is reported as 5 sec. The O<sub>2</sub> analyzer uses a zirconium  
 145 oxide cell with a measurement range of 0 to 25% and a reported t<sub>95</sub> of < 10 sec.



146 Figure 1. Dow UAS with Kolibri attached to the undercarriage.

147

148 **Table 2. CEMS Instruments at both Dow locations.**

Gas Measured	Midland CEMS	St. Charles CEMS
O <sub>2</sub>	Gaus Model 4705	ABB/Magnos 106
NO <sub>x</sub>	Thermo Model 42i-HL	ABB/Limas 11

149

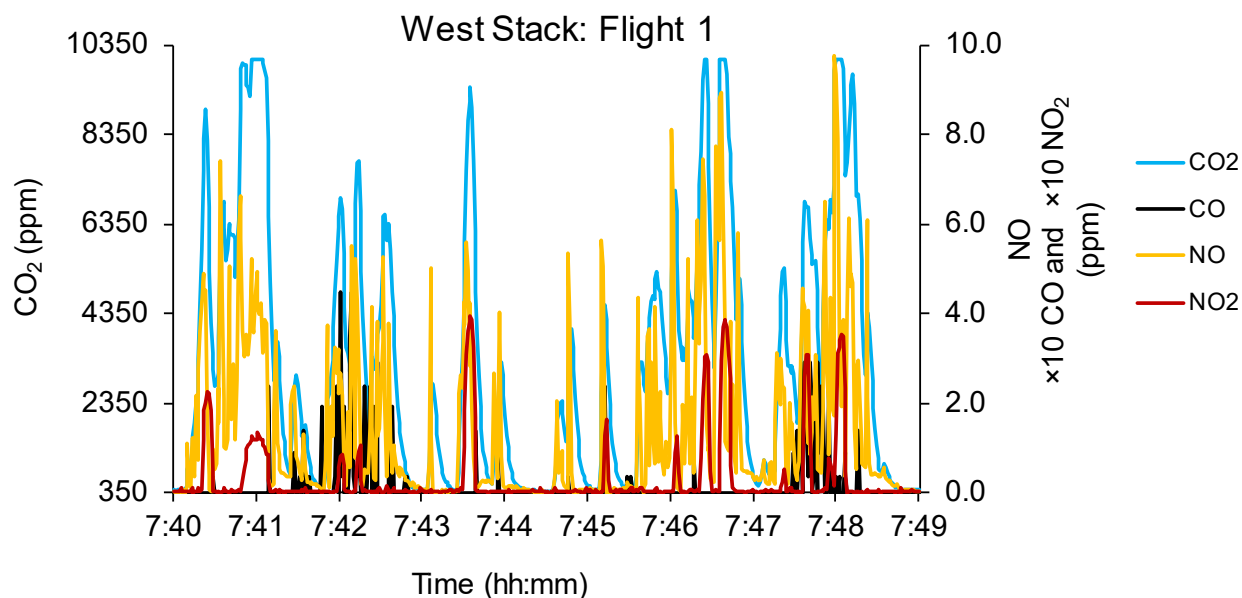
150 The plant CEMS undergo annual relative accuracy audit testing (NSPS Subpart Db, Part 70) using US EPA Method  
 151 7E (2014) for NO<sub>x</sub> and US EPA Method 3A (2017a) for O<sub>2</sub>. Calculation of NO<sub>x</sub> emissions use the appropriate F  
 152 factor, a value that relates the required combustion gas volume to fuel energy input, as described in US EPA Method  
 153 19 (2017b). Flue gas analysis for O<sub>2</sub> and CO<sub>2</sub> are performed in accordance with US EPA Method 3A (2017a) using  
 154 an infrared analyzer to allow for calculation of the flue gas dry molecular weight.

155 The CEMS and UAS/Kolibri data were reduced to a common basis for comparison of results. Emission factors, or  
 156 mass of NO<sub>x</sub> per mass of fuel carbon burned, and emission rates, or mass of NO<sub>x</sub> per energy content of the fuel,  
 157 were calculated from the sample results. The determination of emission factors, mass of pollutant per mass of fuel  
 158 burned, depends upon foreknowledge of the fuel composition, specifically its carbon concentration, and its supply  
 159 rate. The carbon in the fuel is presumed for calculation purposes to proceed to either CO<sub>2</sub> or CO, with the minor  
 160 carbon mass in hydrocarbons and PM ignored for this source type. Concurrent emission measurements of pollutant  
 161 mass and carbon mass (as CO<sub>2</sub> + CO) can be used to calculate total emissions of the pollutant from the fuel using its  
 162 carbon concentration and fuel burn rate.

163 The UAS/Kolibri emission factors were calculated from the mass ratio of NO + NO<sub>2</sub> with the mass of CO + CO<sub>2</sub>  
164 resulting in a value with units of mg NO<sub>x</sub> kg<sup>-1</sup> C. CO<sub>2</sub> concentrations were corrected for upwind background  
165 concentrations. CEMS values of O<sub>2</sub> and fuel flowrate were used to calculate stack flowrate using US EPA Method  
166 19 (2017b). This Method requires the fuel higher heating value and an F factor (gas volume per fuel energy content,  
167 e.g., m<sup>3</sup> kcal<sup>-1</sup> (ft<sup>3</sup> BTU<sup>-1</sup>)) to complete this calculation. For natural gas, the F factor is 967 m<sup>3</sup> 10<sup>-6</sup> kcal (8,710 ft<sup>3</sup> 10<sup>-6</sup>  
168 BTU) (Table 19-2, US EPA Method 19 (2017b)). The concentration, stack flowrate, and fuel flowrate data allow  
169 determination of NO<sub>x</sub> and C emission rates.

### 170 3 Results and Discussion

171 The UAS/Kolibri team easily found the stack plumes at both locations using the wind direction and CO<sub>2</sub> telemetry  
172 data transmitted to the ground operator. Use of an infra-red (IR)/visible camera on a second UAS at St. Charles for  
173 some of the flights aided more rapid location of the plume and positioning of the UAS/Kolibri. Gas concentration  
174 fluctuations were rapid and of high magnitude as observed in a representative trace in Figure 2. CO<sub>2</sub> concentrations  
175 to 10,000 ppm were observed; the relatively lower average CO<sub>2</sub> concentrations reflect the rapid mixing and  
176 entrainment of ambient air causing dilution.



177  
178 **Figure 2. Example of UAS/Kolibri-measured plume concentrations from the St. Charles West Boiler. Data**  
179 **reported at 1 Hz.**

180 Sampling data and emission factors from the UAS/Kolibri are shown in Tables 3, 4, and 5 for the Midland, St.  
181 Charles east stack, and St. Charles west stack, respectively. Eight sampling flights were conducted at the Midland  
182 site, five on the St. Charles East boiler, and nine on the St. Charles West boiler. Both boilers at the Midland site  
183 were operated under the same conditions, so their results have been presented together. Flight times averaged 14 min  
184 (10 % relative standard deviation (RSD)) at the Midland facility and just over 20 min (10 % RSD) at the St. Charles  
185 facility. The shorter flight times in Midland were due to lower UAS battery capacity caused by colder temperatures  
186 (the sampling temperatures in the plume averaged 10±3°C). The average, multi-concentration drift for each of the  
187 sensors, tested at both locations after each sampling day, was less than ±3%. The NO<sub>2</sub>-D4 sensor showed higher  
188 drift (average 8.6%) at one location for the highest concentration of its calibration gas (10.4 ppm). This had minimal  
189 effect on the emission factor calibrations as the measured NO<sub>2</sub> in the plume was actually less than 1 ppm, a range  
190 where the drift was much lower, and NO<sub>2</sub> is a minor contributor to the measured NO<sub>x</sub> species.

191 Average plume NO<sub>x</sub> concentrations were 0.88±0.32 ppm at Midland and 1.22 ppm and 2.41 ppm at the two St.  
 192 Charles boilers with an average RSD of 37 %, 36 %, and 12 %, respectively. The NO emission factor was typically  
 193 97 % of the total NO<sub>x</sub>, with the NO<sub>2</sub> providing the minor balance.

194

195 **Table 3. Midland UAS/Kolibri Sampling Data and Emission Factors.**

Date	Flight #	Flight time (hh:mm:ss)			NO <sub>2</sub> mg kg <sup>-1</sup> C	NO mg kg <sup>-1</sup> C	NO <sub>x</sub> mg kg <sup>-1</sup> C	Avg. CO <sub>2</sub> ppm
		Up	Down	Total				
11/14/2018	1	10:29:00	10:43:00	00:14:00	201	618	819	1213
11/14/2018	2	11:13:04	11:28:28	00:15:24	186	624	810	1138
11/14/2018	3	12:54:17	13:08:47	00:14:30	230	659	889	2948
11/14/2018	5	13:27:40	13:42:05	00:14:25	99	570	669	4658
11/15/2018	6	10:24:20	10:39:30	00:15:10	61	394	454	3703
11/15/2018	7	10:41:36	10:52:40	00:11:04	84	397	481	3983
11/15/2018	8	10:55:10	11:10:10	00:15:00	126	398	524	4781
<b>Average</b>				<b>00:14:13</b>	<b>141</b>	<b>523</b>	<b>664</b>	<b>3203</b>
<b>Stand. Dev.</b>				<b>00:01:28</b>	<b>65</b>	<b>121</b>	<b>179</b>	<b>1514</b>
<b>RSD (%)</b>				<b>10</b>	<b>46</b>	<b>23</b>	<b>27</b>	<b>47</b>

196 Flight # 4 excluded from calculations as CO was observed, which originated from a cycling second boiler.

197

198 **Table 4. St. Charles East Stack UAS/Kolibri Sampling Data and Emission Factors.**

Date	Flight #	Flight time (hh:mm:ss)			NO <sub>2</sub> mg kg <sup>-1</sup> C	NO mg kg <sup>-1</sup> C	NO <sub>x</sub> mg kg <sup>-1</sup> C	Avg. CO <sub>2</sub> ppm
		Up	Down	Total				
07/23/2019	1	09:49:00	10:07:00	00:18:00	1	1442	1442	2305
07/23/2019	2	10:12:00	10:34:00	00:22:00	15	1461	1476	2526
07/23/2019	3	10:45:00	11:08:00	00:23:00	5	1534	1539	785
07/23/2019	4	11:11:00	11:31:00	00:20:00	101	1684	1785	1082
07/23/2019	5	11:52:00	12:01:00	00:09:00	107	2110	2217	1923
<b>Average</b>				<b>00:20:45</b>	<b>30</b>	<b>1530</b>	<b>1560</b>	<b>1675</b>
<b>Stand. Dev.</b>				<b>00:02:13</b>	<b>47</b>	<b>110</b>	<b>155</b>	<b>869</b>
<b>RSD (%)</b>				<b>11</b>	<b>155</b>	<b>7.2</b>	<b>9.9</b>	<b>52</b>

199 *Flight # 5 was not included in the average as elevated CO concentrations were detected, likely from other sources*  
 200 *in the facility.*

201

Date	Flight #	Flight time (hh:mm:ss)			NO <sub>2</sub> mg/kg C	NO mg/kg C	NO <sub>x</sub> mg/kg C	Avg. CO <sub>2</sub> ppm
		Up	Down	Total				
07/24/2019	1	07:31:00	07:49:00	00:18:00	25	1366	1391	3221
07/24/2019	2	07:52:00	08:16:00	00:24:00	49	1263	1312	3503
07/24/2019	3	08:19:00	08:38:00	00:19:00	87	1420	1507	3415
07/24/2019	4	09:23:00	09:46:00	00:23:00	65	1341	1406	4509
07/24/2019	5	09:49:00	10:11:00	00:22:00	47	1296	1343	4813
07/24/2019	6	10:16:00	10:36:00	00:20:00	52	1299	1351	3773
07/24/2019	7	10:38:00	11:00:00	00:22:00	53	1316	1369	4194
07/24/2019	8	11:51:00	12:13:00	00:22:00	90	1460	1549	3129
07/24/2019	9	13:17:00	13:39:00	00:22:00	47	1464	1511	3606
<b>Average</b>				<b>00:21:20</b>	<b>57</b>	<b>1358</b>	<b>1416</b>	<b>3796</b>
<b>Stand. Dev.</b>				<b>00:01:56</b>	<b>21</b>	<b>74</b>	<b>86</b>	<b>586</b>
<b>RSD (%)</b>				<b>9</b>	<b>36</b>	<b>5.5</b>	<b>6.0</b>	<b>15</b>

203

204 Table 6 presents the average O<sub>2</sub> and NO<sub>x</sub> measurement results and the fuel supply rate at both locations. Values for  
 205 natural gas supply, adjusted for the C<sub>2</sub>H<sub>6</sub> and H<sub>2</sub> composition of the St. Charles fuel, were used to calculate the fuel  
 206 carbon supply rate. These data allow calculation of the emission factor, mass of NO<sub>x</sub> to the mass of carbon, reported  
 207 in Table 7.

208

209 **Table 5. Multi-Run Average Stack CEMS Data**

	Midland	St. Charles	
	Both Boilers	East Boiler	West Boiler
O <sub>2</sub> (%)	8.2	4.9	4.5
NO <sub>x</sub> (ppm)	15.7	50.4	42.9
Fuel rate	39.3 10 <sup>6</sup> kJ h <sup>-1</sup>	155.2 10 <sup>6</sup> kJ h <sup>-1</sup>	177.8 10 <sup>6</sup> kJ h <sup>-1</sup>

210

211 **Table 6. Comparison of Average NO<sub>x</sub> Emission Factors from CEMS and UAS/Kolibri**

	Run-Averaged NO <sub>x</sub> Emission Factor, mg NO <sub>x</sub> kg <sup>-1</sup> C (± 1 std dev)		
	Midland	St. Charles	
	Both Boilers	East Boiler	West Boiler
CEMS	612 ± 10	1555 ± 50	1303 ± 29
UAS/Kolibri	664 ± 179	1560 ± 155	1416 ± 86
RPD: CEM & UAS/Kolibri, %	8.2	0.3	8.3

212

213 The UAS/Kolibri NO<sub>x</sub> emission factor for Midland is 8 % higher than the simultaneous CEMS value. For the East  
214 and West boilers at St. Charles, the UAS/Kolibri NO<sub>x</sub> emission factor value is <1 % and 8 % higher, respectively,  
215 than the CEMS values. The difference for the UAS/Kolibri in Midland may be attributed in part to the extremely  
216 cold temperature affecting the performance of the electrochemical sensors. The standard deviations for the CEMS  
217 data are based on the run-average NO<sub>x</sub> values for each test. These values were calculated based on 10 sec averaging  
218 for the Midland tests, 60 sec averaging in St. Charles, and 1 sec averaging for the UAS/Kolibri. Higher standard  
219 deviations for the UAS/Kolibri are predictable given the rapidly changing values and wide range (~0-10 ppm) of  
220 NO<sub>x</sub> data observed in Figure 2. Difference testing for the CEMS and UAS/Kolibri using  $\alpha = 0.05$  and assumed  
221 unequal variances indicate that only the West Boiler and UAS/Kolibri are statistically distinct.

222 The emission rates calculated from the UAS/Kolibri data are 5.6 kg NO<sub>x</sub> • 10<sup>-3</sup> kJ, 14.6 kg NO<sub>x</sub> • 10<sup>-3</sup> kJ, and 13.3 kg  
223 NO<sub>x</sub> • 10<sup>-3</sup> kJ (0.013, 0.034, and 0.031 lbs NO<sub>x</sub> • 10<sup>-6</sup> BTU ), respectively, for the Midland, East St. Charles, and West  
224 St. Charles boilers, below the regulatory standard of 15.5 kg NO<sub>x</sub> • 10<sup>-3</sup> kJ (0.036 lbs NO<sub>x</sub> • 10<sup>-6</sup> BTU). The emission  
225 factors were also calculated as carbon-weighted values to reflect potential differences in plume sampling efficiency  
226 between runs. The Midland, East St. Charles, and West St. Charles UAS/Kolibri emission factors were, respectively,  
227 607, 1525, and 1409 mg NO<sub>x</sub> kg<sup>-1</sup> C. These amounted to relative percent differences of 0.8, 1.9, and 7.8 % between  
228 the CEM and UAS/Kolibri values, for an overall run-weighted average difference of 5.6 %. The difference between  
229 the CEM readings and those from the Kolibri weighted by the carbon collection amounts, reflecting the success at  
230 being within the higher plume concentrations, was 3.5 %.

#### 231 **4 Conclusions**

232 This work reports, to our knowledge, the first known comparison of continuous emission monitoring measurements  
233 made in a stack with downwind plume measurements made using a UAS equipped with emission sensors.

234 The UAS/Kolibri system was easily able to find and take measurements from the downwind plume of a natural gas  
235 boiler despite lack of any visible plume signature. The telemetry system aboard the Kolibri system reported real time  
236 CO<sub>2</sub> concentrations to the operator on the ground, allowing the operator to provide immediate feedback to the UAS  
237 pilot on plume location. Comparison of the CEM data with the UAS/Kolibri data from field measurements at two  
238 locations showed agreement of NO<sub>x</sub> emission factors within 5.6 % and 3.5 % for time-weighted and carbon-  
239 collection-weighted measurements, respectively. This work demonstrates the accuracy of a UAS-borne emission  
240 sampling system for quantifying point source strength. These results also have applicability to area source  
241 measurements, such as open fires, which similarly employ the carbon balance method to determine source strength  
242 emission factors.

243

244 Data availability. The tabular and figure data are available at the Environmental Dataset Gateway  
245 <https://edg.epa.gov/metadata/catalog/main/home.page>.

246

247 Author contributions. BG was the prime author of the paper and the project lead. JA conducted the Kolibri field  
248 testing and data analysis. WM designed the instrument electronics. JR led the UAS group and field test  
249 arrangements.

250

251 Competing interests. The authors declare that they have no conflict of interest.

252

253 Disclaimer. The views expressed in this article are those of the authors and do not necessarily represent the views or  
254 policies of the U.S. EPA.  
255

256 Acknowledgements. Dow's Corporate Aviation Group: Laine Miller, Bryce Young, James Waddell, Jeffrey  
257 Matthews, Chris Simmons, and Anthony DiBiase conducted flights flawlessly. Dow employees Rob Seibert and  
258 Alex Kidd provided technical data and Amy Meskill (Dow), Jennifer DeMelo (Dow), and Dale Greenwell  
259 (EPA/ORD) provided critical logistic support. Patrick Clark (Montrose) reviewed the St. Charles CEMS data.

260  
261 Financial support. This work was supported through a Cooperative Research and Development Agreement between  
262 the U.S. EPA and The Dow Chemical Company.  
263  
264  
265

## 266 **References**

- 267 Aurell, J., W. Mitchell, V. Chirayath, J. Jonsson, D. Tabor, and B. Gullett. Field determination of multipollutant,  
268 open area combustion source emission factors with a hexacopter unmanned aerial vehicle. *Atmospheric*  
269 *Environment* **166**:433-440, DOI: 10.1016/j.atmosenv.2017.07.046, 2017.
- 270 Brady, J. M., M. D. Stokes, J. Bonnardel, and T. H. Bertram. Characterization of a Quadrotor Unmanned Aircraft  
271 System for Aerosol-Particle-Concentration Measurements. *Environmental Science & Technology* **50**:1376-  
272 1383, DOI: 10.1021/acs.est.5b05320, 2016.
- 273 Chang, C.-C., J.-L. Wang, C.-Y. Chang, M.-C. Liang, and M.-R. Lin. Development of a multicopter-carried whole  
274 air sampling apparatus and its applications in environmental studies. *Chemosphere* **144**:484-492, DOI:  
275 10.1016/j.chemosphere.2015.08.028, 2016.
- 276 Craft, T. L. Cahill, C.F.; Walker, G.W. Using an Unmanned Aircraft to Observe Black Carbon Aerosols During a  
277 Prescribed Fire at the RxCADRE Campaign. 2014 International Conference on Unmanned Aircraft  
278 Systems, May 27-30, 2014.
- 279 Li, X. B., D. F. Wang, Q. C. Lu, Z. R. Peng, Q. Y. Fu, X. M. Hu, J. T. Huo, G. L. Xiu, B. Li, C. Li, D. S. Wang, and  
280 H. Y. Wang. Three-dimensional analysis of ozone and PM<sub>2.5</sub> distributions obtained by observations of  
281 tethered balloon and unmanned aerial vehicle in Shanghai, China. *Stochastic Environmental Research and*  
282 *Risk Assessment* **32**:1189-1203, DOI: 10.1007/s00477-018-1524-2, 2018.
- 283 Mori, T., T. Hashimoto, A. Terada, M. Yoshimoto, R. Kazahaya, H. Shinohara, and R. Tanaka. Volcanic plume  
284 measurements using a UAV for the 2014 Mt. Ontake eruption. *Earth Planets and Space* **68**:18, DOI:  
285 10.1186/s40623-016-0418-0, 2016.
- 286 Neumann, P. P., V. H. Bennetts, A. J. Lilienthal, M. Bartholmai, and J. H. Schiller. Gas source localization with a  
287 micro-drone using bio-inspired and particle filter-based algorithms. *Advanced Robotics* **27**:725-738, DOI:  
288 10.1080/01691864.2013.779052, 2013.
- 289 Peng, Z.-R., D. Wang, Z. Wang, Y. Gao, and S. Lu. A study of vertical distribution patterns of PM<sub>2.5</sub>  
290 concentrations based on ambient monitoring with unmanned aerial vehicles: A case in Hangzhou, China.  
291 *Atmospheric Environment* **123**:357-369, DOI: 10.1016/j.atmosenv.2015.10.074, 2015.
- 292 Rosser, K., K. Pavey, N. FitzGerald, A. Fatiaki, D. Neumann, D. Carr, B. Hanlon, and J. Chahl. Autonomous  
293 Chemical Vapour Detection by Micro UAV. *Remote Sensing* **7**:16865-16882, DOI: 10.3390/rs71215858,  
294 2015.
- 295 U.S. EPA Method 7E. Determination of Nitrogen Oxides Emissions from Stationary Sources (Instrumental Analyzer  
296 Procedure). <https://www.epa.gov/sites/production/files/2016-06/documents/method7e.pdf>, 2014, Accessed  
297 August 7, 2019.

- 298 U.S. EPA Method 3A. Determination of oxygen and carbon dioxide concentrations in emissions from stationary  
299 sources (instrumental analyzer procedure). [https://www.epa.gov/sites/production/files/2017-](https://www.epa.gov/sites/production/files/2017-08/documents/method_3a.pdf)  
300 [08/documents/method\\_3a.pdf](https://www.epa.gov/sites/production/files/2017-08/documents/method_3a.pdf) Accessed February 12, 2019, 2017a.
- 301 U.S. EPA Method 19. Determination of sulfur dioxide removal efficiency and particulate matter, sulfur dioxide, and  
302 nitrogen oxide emission rates. [https://www.epa.gov/sites/production/files/2017-](https://www.epa.gov/sites/production/files/2017-08/documents/method_19.pdf)  
303 [08/documents/method\\_19.pdf](https://www.epa.gov/sites/production/files/2017-08/documents/method_19.pdf) Accessed December 6, 2018, 2017b.
- 304 Villa, T. F., F. Salimi, K. Morton, L. Morawska, and F. Gonzalez. Development and Validation of a UAV Based  
305 System for Air Pollution Measurements. *Sensors* **16**, DOI: 10.3390/s16122202, 2016.
- 306 Zhou, X., J. Aurell, W. Mitchell, D. Tabor, and B. Gullett. A small, lightweight multipollutant sensor system for  
307 ground-mobile and aerial emission sampling from open area sources. *Atm. Env.* **154**:31-41, DOI:  
308 10.1016/j.atmosenv.2017.01.029, 2017.